THE JOURNAL OF BIOLOGICAL CHEMISTRY VOL. 287, NO. 13, pp. 10355–10367, March 23, 2012
Published in the U.S.A.

Hepatic Stellate Cell-derived Delta-like Homolog 1 (DLK1) Protein in Liver Regeneration*[S]

Received for publication, October 12, 2011, and in revised form, January 9, 2012 Published, JBC Papers in Press, February 1, 2012, DOI 10.1074/jbc.M111.312751

Nian-Ling Zhu[‡], Kinji Asahina[‡], Jiaohong Wang[‡], Akiko Ueno[‡], Raul Lazaro[‡], Yuichiro Miyaoka[§], Atsushi Miyajima[§], and Hidekazu Tsukamoto[‡¶1]

From the [‡]Southern California Research Center for Alcoholic Liver and Pancreatic Diseases and Cirrhosis and Department of Pathology, Keck School of Medicine, the University of Southern California, Los Angeles, California 90033, the [§]Institute of Molecular and Cellular Biosciences, the University of Tokyo, 7-3-1 Hongo, Bunkyo-ku, Tokyo 113-8656, Japan, and the [¶]Department of Veterans Affairs, Greater Los Angeles Healthcare System, Los Angeles, California 90073

Background: Hepatic stellate cells (HSCs) are activated in liver regeneration, but its significance is unclear.
Results: DLK is induced in HSC activation. Its neutralization causes HSC quiescence via de-repression of *Pparγ* and attenuates liver regeneration.
Conclusion: DLK1 activates HSCs via Wnt pathway and epigenetic repression of *Pparγ* to contribute to liver regeneration.
Significance: A novel role of DLK1 in liver regeneration is identified.

Hepatic stellate cells (HSCs) undergo myofibroblastic activation in liver fibrosis and regeneration. This phenotypic switch is mechanistically similar to dedifferentiation of adipocytes as such the necdin-Wnt pathway causes epigenetic repression of the master adipogenic gene *Pparγ*, to activate HSCs. Now we report that delta-like 1 homolog (DLK1) is expressed selectively in HSCs in the adult rodent liver and induced in liver fibrosis and regeneration. *Dlk1* knockdown in activated HSCs, causes suppression of *necdin* and *Wnt*, epigenetic derepression of *Pparγ*, and morphologic and functional reversal to quiescent cells. Hepatic *Dlk1* expression is induced 40-fold at 24 h after partial hepatectomy (PH) in mice. HSCs and hepatocytes (HCs) isolated from the regenerating liver show *Dlk1* induction in both cell types. In HC and HSC co-culture, increased proliferation and *Dlk1* expression by HCs from PH are abrogated with anti-DLK1 antibody (Ab). *Dlk1* and *Wnt10b* expression by Sham HCs are increased by co-culture with PH HSCs, and these effects are abolished with anti-DLK Ab. A tail vein injection of anti-DLK1 Ab at 6 h after PH reduces early HC proliferation and liver growth, accompanied by decreased *Wnt10b*, nonphosphorylated β-catenin, p-β-catenin (Ser-552), cyclins (cyclin D and cyclin A), cyclin-dependent kinases (CDK4, and CDK1/2), p-ERK1/2, and p-AKT. In the mouse developing liver, HSC precursors and HSCs express high levels of *Dlk1*, concomitant with *Dlk1* expression by hepatoblasts. These results suggest novel roles of HSC-derived DLK1 in activating HSCs via epigenetic *Pparγ* repression and participating in liver regeneration and development in a manner involving the mesenchymal-epithelial interaction.

Hepatic stellate cells (HSCs)[2] constitute a unique type of liver mesenchymal cells with multiple physiological functions. They serve as sinusoidal pericytes, a major site of vitamin A storage, a source of normal extracellular matrix components, and a mesenchymal cell type responsible for mesenchymal-epithelial (hepatocytes) interactions in the liver (1). Upon liver injury, HSCs undergo a phenotypic switch called myofibroblastic transdifferentiation or activation, acquiring the ability to express chemokines and adhesion molecules, participate in extracellular matrix remodeling and deposition, and cause liver fibrosis (1, 2). Numerous proteinaceous, lipid, gaseous mediators arising from neighboring, infiltrating, and its own cells, have been identified to contribute to different aspects of activation mechanisms. Fundamentally, HSC activation must be considered as a consequence of altered cell fate regulation as seen in the framework of cell lineage developments of multipotent mesenchymal progenitor cells to osteoblasts, chondrocytes, smooth muscle cells, adipocytes, and neuron, as well as transdifferentiation among these cell types under changes in their microenvironments. Indeed, our research demonstrates that adipogenic transcription regulation is required for HSC differentiation (3, 4), and a loss of this regulation underlies HSC transdifferentiation into myofibroblastic cells (4, 5) where canonical Wnt signaling is shown to play a major role (6) much like in inhibition of adipogenesis (7). Central to this adipogenic regulation is PPARγ, the master regulator of adipogenesis which is essential for HSC differentiation or quiescence (3, 4). Our recent study demonstrates necdin, a nuclear protein that is known to regulate neuronal, muscle, and preadipocytic differentiation, is selectively expressed in HSCs and induced in activation (8). Further, necdin up-regulates *Wnt10b*, one of the major canonical Wnts expressed by activated HSCs via its bind-

* This work was supported, in whole or in part, by National Institutes of Health Grants P50AA011999 (to H. T.), R24AA012885 (to H. T.), U01AA018663 (to H. T.), RC2AA019392 (to H. T.), and R01AA020753 (to K. A.). This work was also supported by the Medical Research Service of the Department of Veterans Affairs (to H. T.).

[S] This article contains supplemental Fig. S1.

[1] To whom correspondence should be addressed: Dept. of Pathology, Keck School of Medicine, University of Southern California, 1333 San Pablo St., MMR-402, Los Angeles, CA 90033-9141. Tel.: 323-442-5107; Fax: 323-442-3126; E-mail: htsukamo@usc.edu.

[2] The abbreviations used are: HSC, hepatic stellate cell; ALCAM, activated leukocyte cell adhesion molecule; CCl_4, carbon tetrachloride; CDK, cyclin-dependent kinase; Coll-GFP, collagen promoter-GFP; DLK1, delta-like 1 homolog; E, embryonic day; HC, hepatocyte; MeCP2, methyl CpG-binding protein 2; PH, partial hepatectomy; PPARγ, peroxisome proliferator-activated receptor γ; αSMA, α-smooth muscle actin.

ing to the most proximal GN box within the promoter (8). Activated canonical Wnt signaling in turn leads to epigenetic repression of *Pparγ* involving the binding of the methyl CpG-binding protein 2 (MeCP2) to the *Pparγ* promoter and increased H3K27dimethylation at the *Pparγ* exon (9), leading to the loss of this critical adipogenic gene expression and consequent HSC cell fate alteration into myofibroblastic cells (8).

Activated HSCs also support liver regeneration via release of mitogens such as hepatocyte growth factor (10), pleiotrophin (11), and epimorphin (12). Liver regeneration induced by partial hepatectomy (PH) is associated with the loss of HSC-associated vitamin A content (13) and up-regulation of the HSC activation markers such as α-smooth muscle actin (αSMA), IL-6, and hepatocyte growth factor (14), suggesting that HSCs undergo activation and support a regenerative response. Regulation of HSC myofibroblastic activation by the neurotrophin receptor p75NTR is actually crucial for supporting liver regeneration (10). p75NTR is selectively expressed by HSCs and induced in myofibroblastic HSCs. In p75NTR-deficient mice, liver injury resulting from plasminogen deficiency is exacerbated due to insufficient hepatocyte regeneration resulting from deficient hepatocyte growth factor release by HSCs despite suppressed collagen and αSMA expression (10). Thus, activation of HSCs has both fibrogenic and proregenerative purposes, and the best therapeutic strategy for liver disease should be aiming at inhibiting the former while promoting the latter. Adding to this complexity is the role of activated HSCs in liver oncogenesis which commonly accompanies liver fibrosis and cirrhosis. Activated HSCs produce tumor stroma (15) and promote tumor metastasis (16) and progression (15) where active cross-talk between tumor cells and HSCs is implicated (17).

Delta-like 1 homolog (DLK1/Pref-1) is a single-span transmembrane protein with its extracellular domain composed of six epidermal growth factor (EGF)-like repeats. It belongs to the EGF family of homeotic proteins which includes Notch receptors and their ligands known to regulate cell fate and differentiation. DLK1 regulates several differentiation processes including adipogenesis (18–21), osteogenesis (22, 23), neuronal (24), and neuroendocrine (25) differentiation. It is also expressed in malignancies (26) and embryonic hepatoblasts (27) and promotes neuroblastoma cell stemness and tumorigenicity in a manner responsive to hypoxia (28). An extracellular region can be cleaved by the metalloproteinase ADAM-17 (TNF-α-converting enzyme, TACE) to release a soluble 50-kDa protein with biological activity (29). Molecular mechanisms by which DLK1 signals to achieve these biological effects are still elusive. DLK1 may interact with Notch to modulate its signaling (30) or IGF-binding protein 1 to modulate IGF local adipogenic action (31). DLK1 is also recently shown to bind fibronectin and trigger integrin-mediated signaling such as FAK-Rac-ERK activation to inhibit adipogenesis (32).

The present study has identified selective expression of *Dlk1* by HSCs among adult liver cells and its up-regulation in HSC activation *in vitro* and in experimental liver fibrosis and regeneration. DLK1 activates HSCs via epigenetic repression of *Pparγ* in a manner dependent on canonical Wnt. *Dlk1* expression in HSCs is under the control of positive cross-interactions with other morphogens such as Wnt, necdin, and Shh, and most importantly, *Dlk1* up-regulated in liver regeneration after PH supports early hepatocyte proliferation and liver growth via a mechanism which appear to involve *Wnt10b*.

MATERIALS AND METHODS

Animal Models, Cell Isolation and Culture, BrdU Incorporation—HSCs were isolated from male Wistar rats with or without experimental liver fibrosis or mice following PH as described previously (33) by the Non-Parenchymal Liver Cell Core of the Southern California Research Center for ALPD and Cirrhosis. Liver fibrosis was induced in rats by 10-day cholestasis due to ligation of the common bile duct or by provision of phenobarbital in drinking water (500 mg/liter) plus subcutaneous injection of CCl_4 (1 μl/g of body weight) given as a 2-fold dilution with mineral oil twice a week for 3 weeks. Male C57BL/6 mice were subjected to 70% PH, and liver RNA was extracted at 1, 2, 4, 8, and 24 h, as well as every day afterward until the 7th day. HSCs and hepatocytes were isolated 1 day after PH. Mice subjected to 70% PH were also injected via tail vein with anti-DLK antibody or normal rabbit IgG (Abcam) in saline (27 μg/100 μl per mouse) at 6 h after PH to determine the effects on liver growth and biochemical parameters. BrdU was diluted with PBS and injected intraperitoneally to mice 5 h before sacrifice at 1, 2, and 3 days after PH. Frozen liver sections were made, and BrdU immunohistochemistry staining was performed with the BrdU *in Situ* Detection kit (BD Pharmingen). The collagen promoter-GFP (Coll-GFP) transgenic mice obtained from Dr. David Brenner's laboratory at University of California San Diego were also used for isolation of liver mesenchymal cells from E13.5 embryonic or adult livers (34). The use of animals for this study was approved by the Institutional Animal Care and Use Committee of the University of Southern California and Department of Veterans Affairs Greater Los Angeles Healthcare System. HSCs were cultured on plastic with low glucose DMEM supplemented with 10% fetal bovine serum (FBS) and antibiotics for 1 day or 7 days for analysis of quiescent or activated HSCs. HSCs from the liver fibrosis models were cultured on plastic in the medium containing 2% FBS and analyzed immediately after overnight culture. Cell morphology was assessed by phase contrast microscopy, intracellular vitamin A content by UV-excited autofluorescence, and intracellular lipid by Oil Red O staining. For promoter analysis via transient transfection, the spontaneously immortalized cell line (BSC) established from experimental cholestatic liver fibrosis (35) or Huh7 hepatoma cell line was used. Kupffer cells were isolated by an essentially identical procedure except for the use of the cells at the arabinogalactan gradient interface of 1.043/1.058 and 1.058/1.075 and subsequent adherence method as described previously (36). Hepatocytes were isolated by the standard method of *in situ* collagenase digestion of the liver and low speed centrifugation (50 × *g*, 1 min). Sinusoidal endothelial cells were isolated by magnetic cell sorting using SE-1 antibody as described previously (37). Purity and viability of the cells isolated exceeded 95% for all cell types. NIH3T3L1 cells were treated with the adipocyte differentiation mixture MDI (0.5 mM isobutylmethylxanthine, 1 μM dexamethasone, and 1 μM insulin) or dimethyl sulfoxide as a solvent and used for analysis.

Immunohistochemistry—Paraffin-embedded sections of chicken embryos at E6 were obtained from the laboratory of Dr. C.-M. Chuong of the University of Southern California for immunostaining performed by the Morphology Core of the Southern California Research Center for ALPD and Cirrhosis using anti-desmin (Sigma), anti-αSMA (Sigma), and anti-DLK1 (Abcam) antibodies. Mouse embryos or adult livers were fixed with 4% paraformaldehyde, and cryosections (7 μm) were subjected to immunohistochemistry using antibodies against DLK1 (1/1,000; MBL or Abcam), albumin (1/3,000; Nordic), ALCAM (1/100; eBioscience), desmin (1/400; Thermo Scientific), p75NTR (1/1,000; Abcam), αSMA (1/100; Abcam), or Wilms tumor 1 (WT1, 1/50; Cell Marque) as described previously (38). The primary antibodies were detected with secondary antibodies conjugated with Alexa Fluor 488 or 568 (Invitrogen). The sections were counterstained with DAPI (Invitrogen).

Fluorescence-activated Cell Sorting (FACS)—GFP^+ cells were sorted from E13.5 embryos or adult livers of the Coll-GFP mice by FACS as described previously (38). The E13.5 embryonic livers were digested with trypsin-EDTA. The nonparenchymal cells (NPCs) were obtained from the adult livers by the collagenase perfusion method (8). The embryonic liver cells or adult nonparenchymal cells were subjected to FACS using FACS Vantage SE (BD Biosciences) (38). Wild-type mice were used as a negative control.

RNA Extraction and Real Time PCR—Total RNA was extracted from the cells using the RNeasy Mini kit (Qiagen). RNA was reverse-transcribed to cDNA by using a SuperScript III First-strand Synthesis system (Invitrogen) and amplified by 40 cycles using the primers listed below and the SYBR Green PCR Master Mix reagent (AB Applied Biosystems). Each *Ct* value was first normalized to 36B4 *Ct* value and compared between the treatment and control samples. Primer sequences used are: *Pparγ*, 5′-CTG AAG CTC CAA GAA TAC CAAA and 5′-AGA GTT GGG TTT TTT CAG AAT AAT AAGG; *α1(I) collagen*, 5′-TCG ATT CAC CTA CAG CAC GC and 5′-GAC TGT CTT GCC CCA AGT TCC; *Dlk1*, 5′-GGC CAT CGT CTT TCT CAA CA and 5′-ATC CTC ATC ACC AGC CTC CT; *Wnt10b*, 5′-CGA GAA TGC GGA TCC ACAA and 5′-CCG CTT CAG GTT TTC CGT TA; *Wnt3a*, 5′-CAT CGC CAG TCA CAT GCA CCT and 5′-CGT CTA TGC CAT GCG AGC TCA; *necdin*, 5′-TGA TGG TCC GTA TCG ACA AA and 5′-GGA TGT TTC CTG TGC CAG TT; *Shh* 5′-CTG GCC AGA TGT TTT CTG GT and 5′-TAA AGG GGT CAG CTT TTT GG, *36B4*, 5′-TTC CCA CTG GCT GAA AAG GT and 5′-CGC AGC CGC AAA TGC. The primer sequences used in Fig. 6*D* were the same as described previously (38).

Immunoblot Analysis—HSCs were cultured in a 10-cm dish for 7 days followed by infection with Ad.LacZ.shRNA or Ad.Dlk1.shRNA described below at 100 multiplicity of infection for additional 3 days. The cells were then washed with PBS once, and nuclear and cytosolic proteins were isolated as described previously (3). An equal amount of the nuclear or cytosolic extract (20 μg) was separated by SDS-PAGE and electroblotted to nitrocellulose membranes. Antibody against DLK (Abcam), p-AKT, AKT, p-ERK, ERK, p-cMET, or cMET, β-catenin, nonphosphorylated β-catenin, and phospho-Ser-552-β-catenin (Cell Signaling Technology), was incubated with a membrane at a concentration of 0.2–2 μg/10 ml in TBS (100 mM Tris-HCl, 1.5 M NaCl, pH 7.4) with 5% nonfat milk followed by incubation with a horseradish peroxidase-conjugated secondary antibody (Santa Cruz Biotechnology) at 1 μg/10 ml. Proteins were detected by a chemiluminescent method using an ECL kit (Amersham Biosciences).

Construction and Use of Recombinant Adenovirus Vectors—Replication-incompetent recombinant adenovirus expressing necdin shRNA was constructed using the BLOCK-iT Adenoviral RNAi Expression system (Invitrogen) according to the manufacturer's instructions. To select the best shRNA against the rat and mouse *Dlk1* gene, we first designed four shRNA oligonucleotides by using the Invitrogen shRNA designer. Of these, at +375 (5′-GGACGGGAAATTCTGCGAAAT-3′) was shown to be most effective. An additional sequence of CACC was added at the 5′ end, and AAAA was added to the 5′ end of the complementary sequence. These two DNA oligonucleotides were annealed to generate dsDNA, which was subsequently cloned into the pENTR/U6 vector using the BLOCK-iT U6 RNAi Entry Vector kit. The U6 RNAi cassette in the pENTR/U6 necdin shRNA vector was transferred to the adenoviral expression plasmid by LR recombination reaction using Gateway LR Clonase II Enzyme Mix and pAd/BLOCK-iT-DEST Gateway Vector kit. Isolated adenoviral expression clones were then digested with PacI to expose the inverted terminal repeats and transfected into 293A cells using Targefect F-2 (Advanced Targeting Systems) for production of a crude adenoviral stock. Large scale amplification of adenoviral vector was performed in 293A cells as described previously (3, 4). The titer of the purified virus was determined by the standard plaque-forming assay with 293A cells. An adenovirus expressing β-galactosidase shRNA (Ad.LacZ.shRNA) was constructed as a control shRNA vector. Necdin silencing efficiency was tested in day 6 culture-activated rat HSCs with a multiplicity of infection of 50, 100, and 200. Adenovirus expressing GFP, PPARγ, and a dominant negative mutant of PPARγ (gifts from Dr. Krishna K. Chatterjee of the University of Cambridge), or Dkk-1 (a gift from Dr. Calvin Kao, Stanford University), was similarly amplified and purified, and their titers were determined.

Transient Transfection and Reporter Gene Assay—To determine the regulation of DLK1 by necdin, Wnt, or DLK1 itself, the Huh7 human hepatocarcinoma cell line was transiently transfected with the full-length *Dlk1* promoter (−1950/+36)-luciferase construct (a gift from Dr. Sang Hoon Kim, Kyung Hee University, Seoul) by using Targefect F-2 followed 6 h later by infection with Ad.LacZ.shRNA, Ad.necdin.shRNA, or Ad.Dkk1 at 100 multiplicity of infection for 2 days. For *Dlk1* promoter co-transfection assays, the cells were co-transfected with different amounts of a necdin (a gift from Dr. Yoshikawa, University of Osaka) or DLK1-HA expression vector, a LEF or dnTCF expression vector (gifts from Dr. Randall T. Moon, University of Washington, Seattle, WA). For testing the effects of Shh inhibition on DLK1 promoter activity, *Huh7* cells transiently transfected with the promoter-reporter, were treated with different concentrations of cyclopamine for 2 days. The TOPFLASH promoter-luciferase construct (containing eight wild-type T cell factor (TCF)/lymphoid enhancer-binding factor binding

sites, a gift from Dr. Randall T. Moon) was also co-transfected with different amounts of a DLK1 expression vector in Huh7 cells to assess the effects of DLK1 on the canonical Wnt pathway. The cell lysate was collected for determination of both firefly and *Renilla* luciferase activities using the Dual-Luciferase reporter assay system (Promega), and the results were normalized by *Renilla* luciferase activity.

Chromatin Immunoprecipitation (ChIP)—For testing whether DLK1 silencing decreases MeCp2 binding to the *Pparγ* promoter, carrier ChIP was performed using Raji cells as the source of carrier chromatin. For this analysis, Raji cells (1.4×10^7) were added to cultured HSCs (0.2×10^6 cells) with or without DLK1 silencing or Wnt3 or Ad.dnPPARγ treatment and briefly fixed with 1% formaldehyde on the rotating platform for 10 min at room temperature followed by the addition of glycine to a final concentration of 0.125 M. Scraped HSCs and Raji cells in the medium were spun down and washed with cold PBS with protease inhibitors. After lysis of the cells with SDS buffer (1% SDS, 10 mM EDTA, 50 mM Tris-HCl, pH 8.1) with protease inhibitors, the lysate was sonicated and snap-frozen in aliquots. For ChIP, diluted samples were first precleared with protein G-agarose and then incubated with antibody against MeCP2 (Abcam) at 1 μg/μl at 4 °C overnight followed by precipitation with protein G-agarose. After elution of immunoprecipitated complex, cross-linking was reversed with 5 M NaCl and proteins digested with protease K. Extracted chromatin was subjected to real-time PCR using the primers flanking a segment within the *Pparγ* promoter as described recently (9). *Ct* values of the samples with nonimmune IgG were subtracted and compared with their respective input *Ct* values.

Statistical Analysis—All numerical data are expressed as mean ± S.D., and a significance of a difference was determined by a two-tailed *t* test.

RESULTS

Dlk1 Is Selectively Expressed by HSCs in Adult Rat Liver and Induced in HSC Activation—We first examined the expression of *Dlk1* in four different cell types isolated from male adult rat livers by quantitative PCR and immunoblot analyses. *Dlk1* mRNA levels are at least severalfold higher in HSCs than other cell types (Fig. 1*A*). Immunoblot analysis reveals a distinct ~60 kDa band and weaker expression of small molecular species (<50 kDa) in 1 day (D1) quiescent HSCs, but not in sinusoidal endothelial cells or Kupffer cells (Fig. 1*B*). Hepatocytes show a faint expression of these proteins which may be attributable to inevitable contamination of a small percentage of HSCs after the conventional isolation technique (39). Expression of these molecular forms of DLK1 due to alternative splicing and post-translational modifications have been described previously (21, 40, 41), and that with most abundant expression (~60 kDa) is believed to be the full-length form. HSCs which have undergone "activation" after 7-day culture on plastic (D7), show a clear induction of DLK1 much like that seen in 3T3L1 preadipocytic fibroblasts treated with dimethyl sulfoxide. In contrast, adipocytes generated after the treatment of 3T3L1 cells with the adipocyte differentiation mixture MDI, show attenuated expression (Fig. 1*B*). Next, we examined the expression of *Dlk1* in activated HSCs isolated from rats with experimental liver

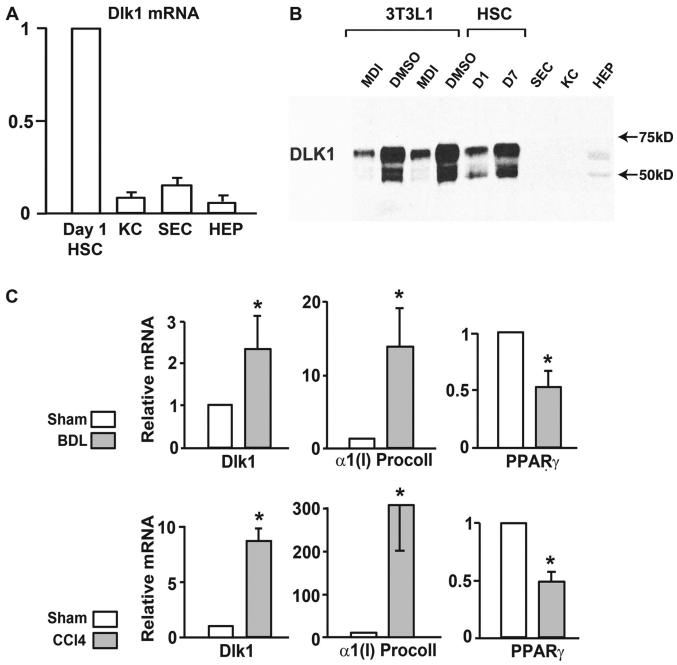

FIGURE 1. *A*, quantitative PCR analysis for *Dlk1* mRNA reveals a selective expression by HSCs compared with Kupffer cells (*KC*), sinusoidal endothelial cells (*SEC*), or hepatocytes (*HEP*) isolated from adult rat livers. *B*, immunoblotting confirms selective expression of DLK1 by day 1 (*D1*) HSCs and demonstrates DLK1 induction in activated HSCs cultured for 7 days on plastic (*D7*). In parallel, DLK1 expression in 3T3L1 preadipocytic fibroblasts (*DMSO*) *versus* adipocytes generated after the MDI treatment (*MDI*) is shown. *C*, *Dlk1* mRNA is induced in HSCs isolated from experimental liver fibrosis induced by bile duct ligation (*BDL*) or repetitive CCl_4 injection. *, $p < 0.05$ compared with respective controls. *Error bars*, S.D.

fibrosis induced by the ligation and scission of the common bile duct or repetitive injection of CCl_4. In both models, isolated HSCs show up-regulation of *Dlk1* mRNA expression along with that of *α1(I) procollagen* with conversely suppressed expression of the HSC differentiation or quiescence gene *Pparγ* (Fig. 1*C*). These results demonstrate that *Dlk1* is selectively expressed in HSCs in the liver and induced in HSC activation *in vitro* and *in vivo*.

Dlk Knockdown Reverses Activated HSCs to Quiescent Cells—We next expressed shRNA against *Dlk1* via an adenoviral vector in culture-activated HSCs to determine the role of *Dlk1* in cell fate regulation. In 48~72 h after infection with the adenovirus expressing the shRNA (Ad.Dlk1.shRNA), expression of the major full-length DLK1 is reduced by 60~70% compared with the cells infected with the control virus expressing shRNA against *LacZ* (Ad.LacZ.shRNA) (Fig. 2*A*). This manipulation reverses the phenotype of activated cells to that of quiescent or differentiated HSCs with an increased content of intracellular vitamin A as assessed by UV-excited vitamin A autofluorescence and increased lipid content detected by Oil Red O staining (Fig. 2*B*). This morphologic reversal is accompanied by suppressed expression of the genes associated with HSC activation such as *necdin* (Ncd), *α1(I) procollagen* (Coll), canonical Wnts (*Wnt10b* and *Wnt3a*), and *Shh* but increased expression of the quiescence genes such as *Pparγ* and *C/ebpα* (Fig. 2*C*). We further tested the regulatory role of DLK1 in canonical Wnt signaling by testing the effects of a DLK1 expression vector on the TOPFLASH promoter activity. For this experiment, we used Huh7 cells because activated HSCs or HSC line already express

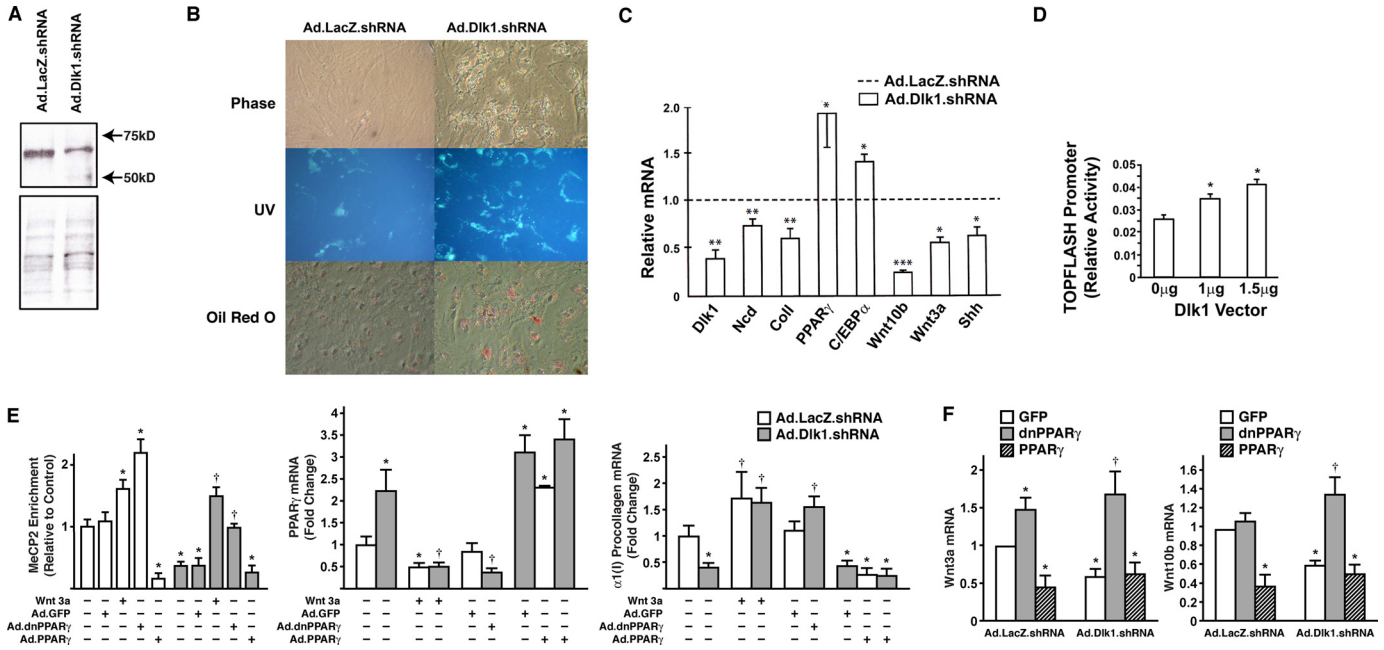

FIGURE 2. *A*, DLK1 knockdown shown by immunoblotting (*upper panel*), which is achieved by an adenovirus expressing shRNA against *Dlk1* (Ad.Dlk1.shRNA) *versus* a control vector expressing shRNA against LacZ (Ad.LacZ.shRNA). *Lower panel* is Ponceau staining of loaded proteins. *B*, *Dlk1* knockdown with Ad.Dlk1.shRNA achieves a morphologic reversal of culture-activated rat HSCs to a quiescent phenotype with increased vitamin A content as shown by UV-excited autofluorescence and increased lipid content shown by Oil Red O staining. *C*, *Dlk1* knockdown up-regulates adipogenic genes, *Pparγ* and *C/ebpα* while down-regulating the activation markers such as *necdin* (Ncd), *α1(I) procollagen* (Coll), canonical *Wnt10b* and *Wnt3a*, and *Shh*. *, $p < 0.05$; **, $p < 0.01$; ***, $p < 0.005$ compared with the cells infected with Ad.LacZ.shRNA. *Error bars*, S.D. *D*, DLK1 expression increases TOPFLASH promoter activity in Huh7 cells transiently transfected with the promoter-luciferase construct and a DLK1 expression vector. *, $p < 0.05$ compared with the basal promoter activity. *E*, Wnt3a addition or dnPPARγ expression increases MeCP2 binding to the *Pparγ* promoter whereas PPARγ expression reduces it. *Dlk1* knockdown (Ad.Dlk1.shRNA) reduces MeCP2 enrichment to the *Pparγ* promoter, restores *Pparγ* mRNA expression, and down-regulates *α1(I) procollagen* expression. But these effects are abrogated by addition of Wnt3a or expression of a dominant negative mutant of *Pparγ* (Ad.dnPPARγ). PPARγ expression by an adenoviral vector (Ad.PPARγ) is equally effective in inhibiting MeCP2 binding and *α1(I) procollagen* expression but does not render an additive effect on suppression of these parameters achieved by *Dlk1* knockdown. *, $p < 0.05$ compared with the cells infected with Ad.LacZ.shRNA or Ad.GFP; †, $p < 0.05$ compared with the level seen with Ad.Dlk1.shRNA without Wnt3a or with Ad.GFP. *F*, reduced expressions of Wnt3a and Wnt10b by *Dlk1* knockdown are abrogated by expression of dnPPARγ. PPARγ expression reduces Wnt3a and Went10b to the levels achieved by *Dlk1* knockdown but no additive effect when combined with *Dlk1* knockdown. *, $p < 0.05$ compared with Ad.LacZ.shRNA or Ad.GFP; †, $p < 0.05$ compared with Ad.Dlk1.shRNA without Wnt3a addition or with the control GFP expression.

high levels of DLK1. As shown in Fig. 2*D*, the TOPFLASH activity is significantly increased by the expression of DLK1. Combined with the results on the effects of *Dlk1* knockdown, these data demonstrate the positive regulation of the canonical Wnt pathway by DLK1.

Dlk1 Knockdown Epigenetically Derepresses Pparγ in Manner Dependent on Wnt Suppression and PPARγ Activity—Activation of HSCs is caused by the loss of *Pparγ* expression, and ectopic *PPARγ* expression in activated HSCs restores their quiescence (3, 4). The loss *Pparγ* expression is due to the epigenetic repression mediated by MeCP2 (8, 9). MeCP2 orchestrates heterochromatin formation at the *Pparγ* locus by not only binding to the promoter and recruiting HDAC and the co-repressor HP-1α, but also up-regulating EZH2 and increasing H3K27di- or trimethylation at the 3′ exons (8, 9). As expected from our previously study (8), Wnt3a addition further increases MeCP2 enrichment to the *Pparγ* promoter in culture-activated HSCs (Fig. 2*E*, *left panel*, *3rd bar versus 1st bar*). Expression of a dominant negative mutant of PPARγ by an adenoviral vector (Ad.dnPPARγ) also increases the enrichment (*4th versus 2nd bar*) whereas expression of PPARγ (Ad.PPARγ) effectively suppresses it (*5th versus 2nd* bar), suggesting the importance of intact PPARγ activity in preventing MeCP2-mediated epigenetic repression of *Pparγ*. Next, we determined whether the restored *Pparγ* expression and HSC phenotypic reversal by *Dlk1* knockdown are accompanied by reduced MeCP2 binding to the promoter. Indeed, the *Dlk1* knockdown significantly reduces MeCP2 enrichment to the promoter (*6th versus 1st bar*). Because *Dlk1* knockdown suppresses canonical Wnts (Fig. 2*C*) which mediate *Pparγ* epigenetic repression (8), we asked whether reduced MeCP2 enrichment by the knockdown is abrogated by addition of exogenous Wnt3a. This treatment indeed blocks the reduction in MeCP2 binding and even increases it over the control level (*8th versus 6th bar*), suggesting that the epigenetic derepression is dependent on Wnt suppression. Next, we examined the effects of Ad.dnPPARγ and Ad.PPARγ with *Dlk1* knockdown. Overexpression of dnPPARγ but not wild-type PPARγ prevents the reduction in MeCP2 binding achieved by *Dlk1* knockdown, suggesting that this derepression effect is also dependent on intact PPARγ activity. Parallel analysis for *Pparγ* and *α1(I) procollagen* mRNA levels demonstrate that restored expression of *Pparγ* and suppressed *α1(I) procollagen* expression by *Dlk1* knockdown are also blocked by Wnt3a addition or dnPPARγ expression (Fig. 2*E*, *middle* and *right panels*). Ad.PPARγ raises *Pparγ* mRNA to the level achieved by *Dlk1* knockdown and reduces *procollagen* expression as achieved by *Dlk1* knockdown (the *last three bars* of Fig. 2*E*, *middle* and *right panels*). To examine a potential link between Wnt suppression and PPARγ activity which are both required for the derepression the *Pparγ* gene, we assessed the

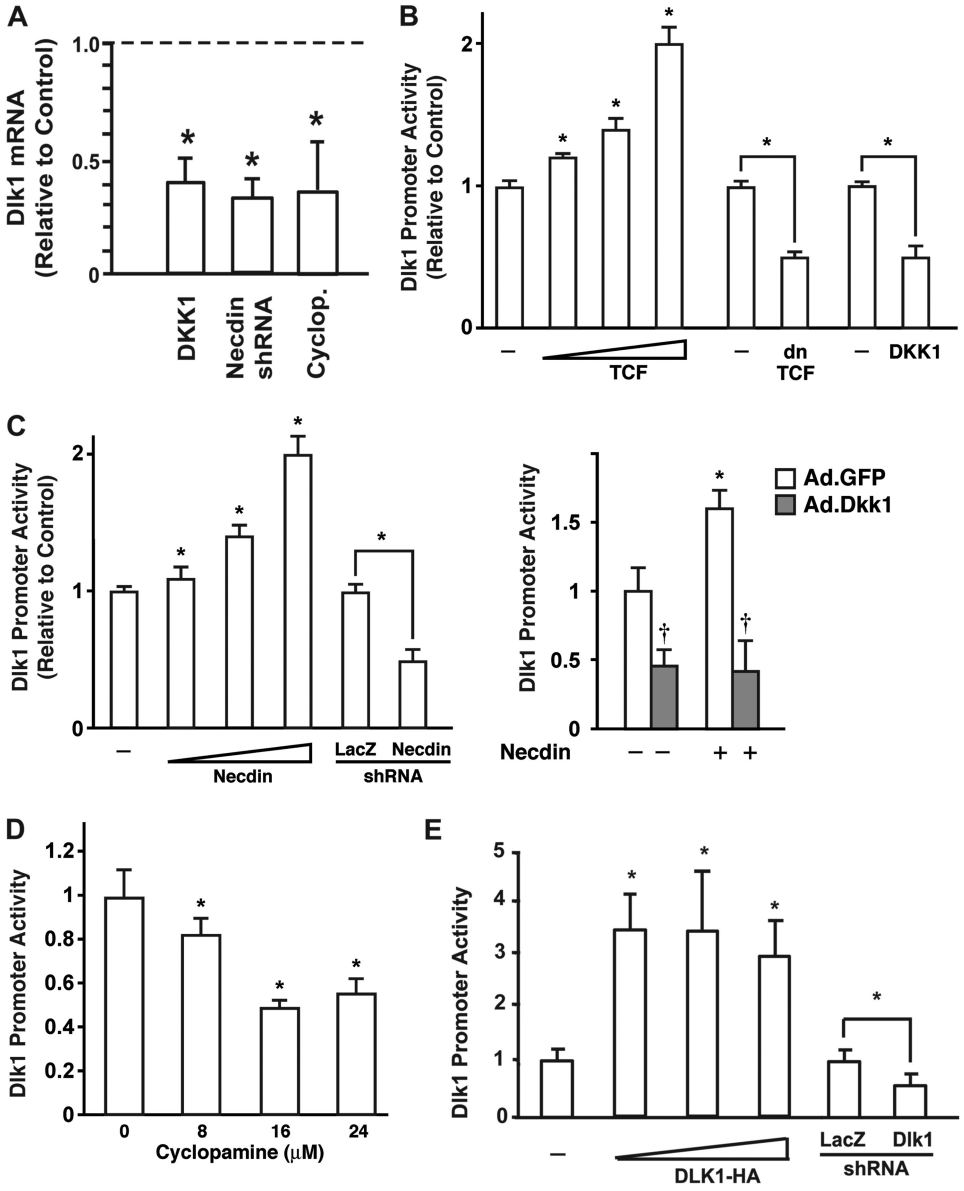

FIGURE 3. *A*, *Dlk1* mRNA expression is reduced by expression of the Wnt co-receptor antagonist DKK1 or necdin shRNA expressed by an adenovirus, or by treatment with cyclopamine (16 μM). *, $p < 0.05$ compared with the respective control which is indicated by a *dotted line*. *B*, *Dlk1* promoter activity as assessed by a transient transfection of the BSC line with *Dlk1* promoter-luciferase, is up-regulated by TCF expression (0.5∼1.5 μg of TCF plasmid) but reduced by expression of a dominant negative TCF (dnTCF), or DKK1. *, $p < 0.05$ compared with the basal promoter activity. *C*, Dlk1 promoter activity in Huh7 cells is increased by expression of necdin (0.25∼1 μg of plasmid) but reduced by necdin shRNA (*left panel*). Because necdin is overexpressed in the BSC line, we used Huh7 cells to examine the effect of necdin expression. Expression of the Wnt antagonist Dkk1 abrogates necdin-induced *Dlk1* promoter activity and reduces the basal promoter activity (*right panel*). *, $p < 0.05$ compared with the basal promoter activity. †, $p < 0.05$ compared with the cells infected with Ad.GFP. *D*, *Dlk1* promoter activity is reduced by the Shh inhibitor cyclopamine in the BSC line. *, $p < 0.05$ compared with the basal activity. *E*, *Dlk1* promoter activity is increased by DLK1 expression (62.5∼250 ng of DLK1-HA plasmid) and reduced by *Dlk1* knockdown with shRNA in Huh7 cells. Huh7 cells were used due to relatively lower expression of DLK1 compared with the BSC line. *, $p < 0.05$ compared with the basal promoter activity. *Error bars*, S.D.

effects of dnPPARγ on the expression of canonical Wnt3a and Wnt10b. As predicted, *Dlk* knockdown down-regulates both *Wnt3a* and *Wnt10b*, but dnPPARγ overexpression completely abrogates this effect (Fig. 2*F*), suggesting that PPARγ activity itself down-regulates the canonical *Wnts* which are inducible by DLK1. In support of this notion, expression of PPARγ reduces both Wnt3a and Wnt10b to the level achieved with *Dlk* shRNA, and a combination of *Dlk* knockdown and PPARγ expression does not have an additive effect, suggesting that PPARγ expression which is maximally restored by *Dlk* knockdown, renders maximal inhibition of Wnt expression. Collectively, these results suggest that DLK1 negatively regulates expression of PPARγ via epigenetic repression and up-regulates canonical Wnt expression by reducing PPARγ-mediated inhibition.

Dlk1 under Control of Cross-interactions with Other Morphogens—We next examined how *Dlk1* expression in HSCs is regulated by other morphogens such as *Wnts*, *necdin*, and *Shh* shown to be involved in activation of HSCs (6, 8, 42). In day 7 culture-activated HSCs, *Dlk1* mRNA expression is suppressed by inhibition of canonical Wnt signaling with the Wnt co-receptor antagonist Dickkopf-1 (DKK1), *necdin* shRNA,

and the Shh inhibitor cyclopamine (Fig. 3*A*). *Dlk1* promoter activity is up-regulated by expression of TCF and inhibited by expression of dnTCF or the Wnt co-receptor antagonist DKK1 (Fig. 3*B*) in the activated HSC line BSC, suggesting that the canonical Wnt signaling induces *Dlk1* expression via its promoter activation. *Dlk1* promoter is similarly activated by necdin and reduced by *necdin* shRNA (Fig. 3*C*). Because our earlier work identifies necdin as a positive regulator of Wnt10b transcription (8), we next tested whether necdin-induced *Dlk1* promoter activation is dependent on the canonical Wnt pathway. Indeed, necdin-induced promoter activity is completely abrogated by expression of DKK1 (Fig. 3*C*, *right panel*). In fact, DKK1 even suppresses the basal promoter activity, suggesting the activity of endogenous necdin in activating the Wnt pathway and *Dlk1* promoter. Cyclopamine also suppresses *Dlk1* promoter activity (Fig. 3*D*). Collectively, these results suggest that *Dlk1* is under a positive regulation by Wnt, necdin, and Shh. Because *Dlk1* knockdown also reduces the expression of Wnt10b, Wnt3a, necdin, and Shh (Fig. 2*C*), there appear to be positive cross-interactions between DLK1 and other morphogens. In addition, DLK1 also has a self-inductive effect as DLK1 expression induces and DLK1 knockdown reduces the *Dlk1* promoter activity (Fig. 3*E*).

Dlk1 Up-regulation in Liver Regeneration—Compelling evidence suggests that activated HSCs participate in liver regeneration. To test the potential role of HSC-derived DLK1 in liver regeneration, we first examined the expression of *Dlk1* mRNA in total RNA extracted from mouse regenerating livers during the first 24 h and a subsequent 7-day period after 70% PH. *Dlk1* expression is very low before PH and gradually up-regulated >40-fold at 24 h, and this induction takes place after inductions of known mitogen and co-mitogen genes such as *Hgf*, *Tnfα*, and *Il6* at 1~4 h after PH (Fig. 4*A*, *left*). The *Dlk* message is reduced toward the basal level at day 3–7 (Fig. 4*A*, right). Induction of *necdin* and *Wnt10b* begins to occur at day 2–3 and with much lower magnitudes, and *Shh* induction is late at day 7 (Fig. 4*A*). This induction of *Dlk1* at 24 h prompted us to examine HSCs and HCs isolated at this time point. HSCs isolated at 24 h after PH show a >4-fold increase in *Dlk1* mRNA level compared with HSCs isolated at 24 h after Sham operation (Fig. 4*B*). HCs isolated from Sham mice have a very low level of *Dlk1* expression, but it increases significantly in PH animals at 24 h (Fig. 4*B*). These HSCs and HCs were co-cultured immediately after isolation with HSCs on the bottom of the wells and HCs on the insert (Fig. 4*C*). DNA synthesis of HCs was determined by [^{3}H]thymidine incorporation in the absence or presence of anti-DLK1 antibody in the medium. HCs from PH have a significantly increased proliferation compared with Sham HCs. Addition of anti-DLK1 antibody to the culture medium abolishes this increment of PH HC proliferation but has no effect on Sham HCs (Fig. 4*C*). In a separate set of the identical experiment, *Dlk1* mRNA levels were determined in both HSCs and HCs. Induction of *Dlk1* expression in both cell types of PH mice is completely abrogated with the anti-DLK1 antibody (Fig. 4*D*), suggesting the existence of autocrine and paracrine loops.

Next, we tested the effects of the neutralizing antibody in the PH model *in vivo*. For this experiment, the antibody or an equal amount of nonimmune IgG (27 μg) was injected via tail vein at 6 h after PH, the time point *Dlk1* mRNA begins to increase. Prior to sacrificing, BrdU was injected for subsequent assessment of HC DNA synthesis by immunohistochemistry. BrdU incorporation into PH HCs is consistently lower at days 1, 2, and 3 in the animals treated with anti-DLK1 antibody than those with injection of nonimmune IgG (Fig. 4*E*). The liver growth as assessed by a fraction of liver weight over body weight is also reduced by the neutralizing antibody treatment at day 1 ($p < 0.05$) and day 2 ($p = 0.05$ using a two-tailed t test), but a significant difference is not observed at days 3 and 7 (Fig. 4*F*). These inhibitory effects on liver regeneration are associated with suppressed expression of *Dlk1* (supporting anti-DLK1 antibody sufficiently blocked self-induction), *p75Ntr*, *Wnt10b*, and *Ptn* mRNA but not *Tnfa*, *Il6,* and *Hgf* (Fig. 5*A*); decreased G_1 (cyclin D) and S (cyclin A) phase cyclines and their partner cyclin-dependent kinases (CDK4 and CDK1/2), as well as suppressed levels of p-ERK1/2 and p-AKT at days 1, 2, and/or 3 as highlighted by *boxed blots* in Fig. 5*B*. These results suggest that DLK1 induced in both HSCs and HCs after PH, has an important role in inducing growth factor genes such as *Wnt10b*, *Ptn*, or *p75Ntr* and that neutralization of DLK1 results in diminished growth signals and early liver growth after PH. We became particularly interested in *Wnt10b* because it induces canonical Wnt signaling which in turn activates many of cell cycle genes shown to be suppressed by anti-DLK1 antibody. To address this possibility, we examined the protein levels of nonphosphorylated (stabilized) β-catenin and total β-catenin in liver protein extracts of day 2 PH livers. Anti-DLK1 antibody treatment indeed reduces the level of stabilized β-catenin by 75% and total β-catenin modestly (Fig. 5*C*). β-Catenin is phosphorylated at Ser-552 by activated AKT, and this modification increases its nuclear translocation and activity. Because p-AKT is reduced by the antibody treatment (Fig. 5*B*), we thought p-β-catenin (Ser-552) levels may also be reduced. Indeed, p-β-catenin (Ser-552) levels are reduced by 55% by the antibody treatment (Fig. 5*C*). Collectively, these results suggest that the DLK1-Wnt10b-β-catenin pathway contributes to HC proliferation in liver regeneration and that HC DLK1 is induced by HSC-derived DLK1. To test the latter possibility, we have performed a cross-culture experiment in which HCs from Sham were co-cultured with HSCs from Sham or PH. Both *Dlk1* and *Wnt10b* expression are induced in Sham HCs when co-cultured with PH HSCs as opposed to Sham HSCs, and these inductions are abrogated by addition of anti-DLK1 antibody in culture (Fig. 5*D*), supporting the notion that HSC-derived DLK1 mediates a mitogenic response in HCs via the DLK1-Wnt10b pathway.

DLK1 Expression in Mouse Embryonic Liver—DLK1 is known to be expressed by hepatoblasts (27), but our findings in the liver regeneration model suggest that DLK1 may also be expressed by HSCs in developing liver. To examine this question, we first performed immunostaining for DLK1 along with desmin and αSMA on chicken embryonic livers at E5 when the first lobe is developed. Embryonic HSCs which surround islands or codes of hepatoblasts are stained positively for desmin and αSMA (Fig. 6*A*), supporting the notion that embryonic HSCs have an activated phenotype. These HSCs are also positively stained for DLK1. In addition, a subpopulation of

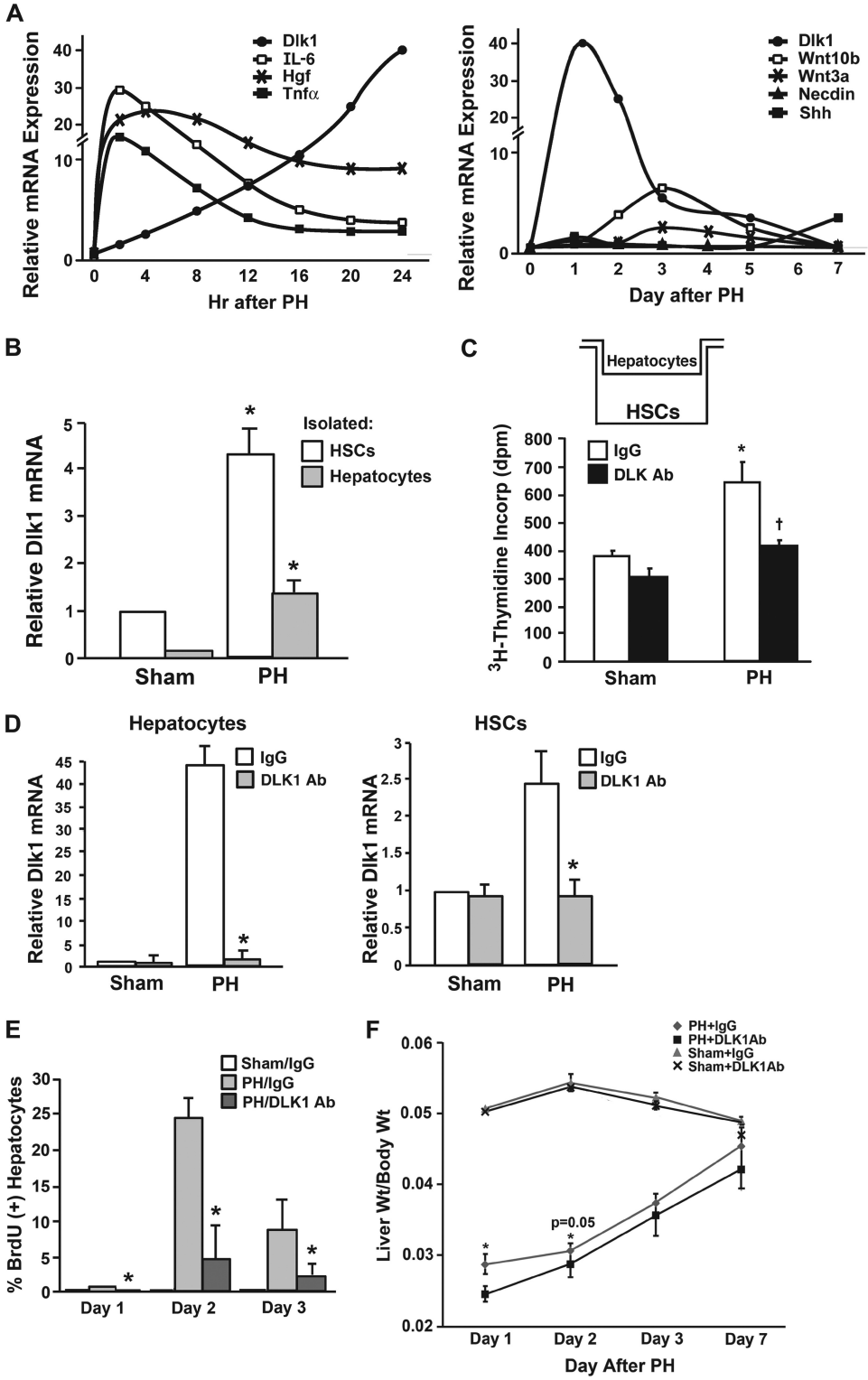

FIGURE 4. *A*, Expression of *Dlk1*, cytokines, and growth factors after PH is shown. Note that *Dlk1* is gradually induced after induction of *Tnfα*, *Il6*, and *Hgf* and peaks at 24 h (*left panel*). *Dlk1* induction is followed by milder up-regulation of Wnt10b and necdin at 2~3 days and that of Shh at day 7. *B*, HCs and HSCs isolated at day 1 after PH were show increases in *Dlk1* mRNA levels in both cell types. *, $p < 0.05$ compared with the respective cells isolated from Sham-operated mice. *C*, HCs and HSCs isolated at day 1 after PH were co-cultured to determine DNA synthesis of HC in the absence or presence of anti-DLK1 antibody. Note that increased DNA synthesis by PH HC is abrogated with anti-DLK1 antibody. *, $p < 0.05$ compared with Sham HC with nonimmune IgG; †, $p < 0.05$ compared with PH HC with nonimmune IgG. *D*, in an experiment identical to that in *C*, *Dlk1* mRNA levels were determined in both cell types. Note that *Dlk1* up-regulation seen in both cell types is completely abrogated by addition of anti-DLK1 antibody. *, $p < 0.05$ compared with the non-IgG treatment. *E*, administration of anti-DLK1 antibody given 6 h after PH significantly attenuating HC DNA synthesis as determined by BrdU incorporation at days 1, 2, and 3 after PH in mice. *, $p < 0.05$ compared with nonimmune IgG treatment in PH mice. *F*, anti-DLK1 antibody treatment described in *E* reducing liver growth as assessed by the liver weight/body weight fraction at day 1 and 2 after PH. *, $p < 0.05$ compared with IgG treatment. *Error bars*, S.D.

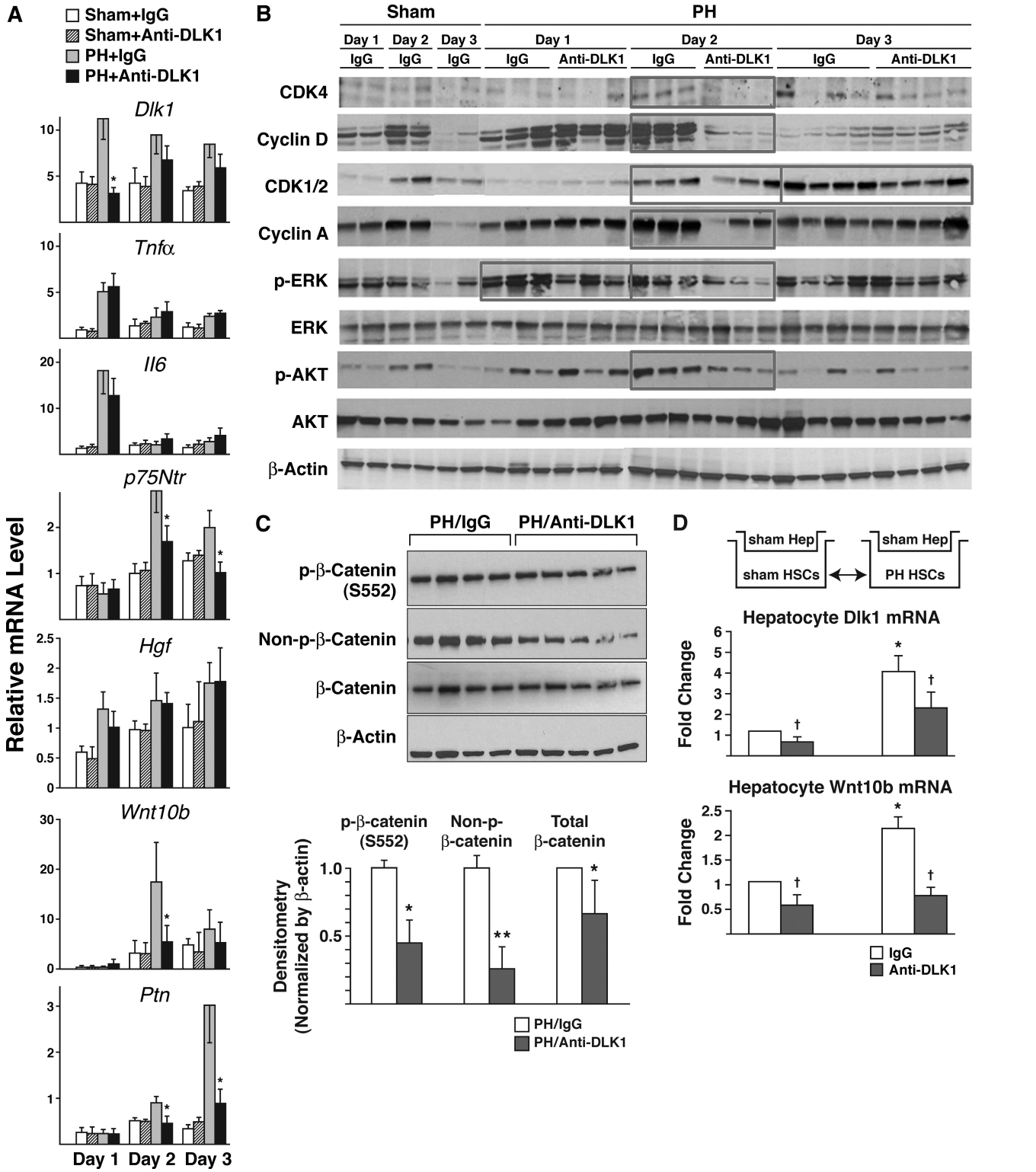

FIGURE 5. *A*, anti-DLK1 antibody treatment as described for Fig. 4*E*, reduces *Dlk1*, *p75Ntr*, *Wnt10b*, and *Ptn* mRNA expression in regenerating livers at day 1, 2, or/and 3 after PH. The levels of mRNA were determined by quantitative PCR of total liver RNA, normalized by the housekeeping gene *m36B4*, and expressed as -fold changes compared with the control values at day 0 (prior to PH). *, $p < 0.05$ compared with those treated with nonimmune IgG (*IgG*). *B*, anti-DLK1 antibody treatment reduces CDK4, cyclin D, CDK1/2, cyclin A, p-ERK1/2, p-AKT on day 2 after PH. Original blots that generated this figure are shown in supplemental Fig. S1. *C*, anti-DLK1 antibody treatment significantly reduces the levels of p-β-catenin (Ser-552), stabilized non-p-β-catenin, and total β-catenin in regenerating livers 2 days after PH as determined by densitometry analysis of immunoblots. *, $p < 0.05$; **, $p < 0.01$ compared with the livers of nonimmune IgG-treated mice. *D*, cross-co-culture experiment with Sham HCs and Sham or PH HSCs reveals induction of HC *Dlk1* and *Wnt10b* expression by PH HSCs which are abrogated with anti-DLK1 antibody, suggesting that HSC-derived DLK1 activates the DLK1-Wnt10b pathway in HC. *, $p < 0.05$ compared with co-culture with Sham HCs; †, $p < 0.05$ compared with IgG treatment. *Error bars*, S.D.

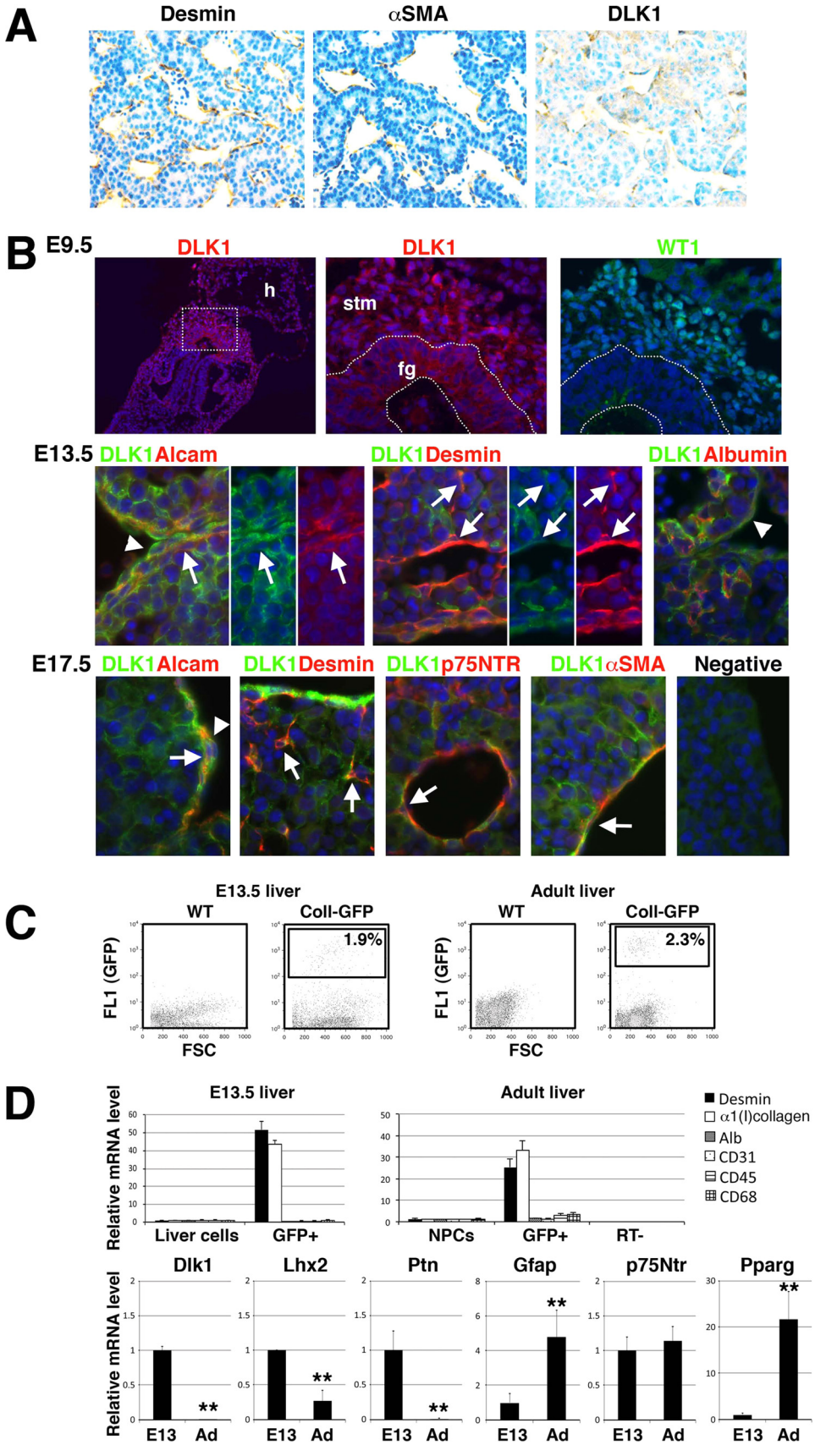
A
Desmin
αSMA
DLK1
B
E9.5
DLK1
DLK1
WT1
h
stm
fg
E13.5
DLK1Alcam
DLK1Desmin
DLK1Albumin
E17.5
DLK1Alcam
DLK1Desmin
DLK1p75NTR
DLK1αSMA
Negative
C
E13.5 liver
Adult liver
WT
Coll-GFP
WT
Coll-GFP
1.9%
2.3%
FL1 (GFP)
FSC
FL1 (GFP)
FSC
D
E13.5 liver
Adult liver
Desmin
α1(I)collagen
Alb
CD31
CD45
CD68
Relative mRNA level
Liver cells
GFP+
NPCs
GFP+
RT-
Dlk1
Lhx2
Ptn
Gfap
p75Ntr
Pparg
Relative mRNA level
**
E13
Ad

hepatoblasts is diffusely positive for DLK1. In mouse embryos at E9.5, the foregut endoderm and $WT1^+$ septum transversum mesenchyme, from which HSCs originate (43), express DLK1 (Fig. 6*B*). At E13.5, in addition to $albumin^+$ hepatoblasts, $ALCAM^+$ mesothelial cells and submesothelial cells, which are recently shown to be the precursor of HSCs (43), express DLK1 at the liver surface (Fig. 6*B*). $Desmin^+$ HSCs and perivascular mesenchymal cells are occasionally positive for DLK1 (Fig. 6*B*). In E17.5 embryos, DLK1 expression decreases in hepatoblasts (Fig. 6*B*) as reported previously (27) and persists in $ALCAM^+$ mesothelial cells and submesothelial cells (Fig. 6*B*). In addition, some $desmin^+$ HSCs and $p75NTR^+$ αSMA^+ perivascular mesenchymal cells clearly express DLK1 in E17.5 livers (Fig. 6*B*). Next, we isolated liver mesenchymal cells using collagen promoter-GFP (Coll-GFP) transgenic mice from E13.5 embryonic or adult livers by FACS (Fig. 6*C*). Because embryonic HSCs are devoid of fat/vitamin A and their specific surface marker is yet to be identified, this GFP^+ cell population, which includes HSCs, submesothelial cells, and perivascular mesenchymal cells, was the best we could study. As shown in Fig. 6*D*, $GFPA^+$ populations from E13.5 and adult livers are enriched with *desmin* and *α1(I) procollagen* (Coll)-expressing cells. Compared with the E13.5 GFP^+ cells, the expression level of *Dlk1* mRNA decreases significantly in the adult GFP^+ cells, similar to *Lhx2* and *Ptn*, genes expressed in fetal liver mesenchymal cells (Fig. 6*D*). Conversely, the expression levels of *Gfap* and *Pparγ* increase in the adult GFP^+ cells. These results demonstrate that DLK1 is expressed in HSC progenitor cells and HSCs as well as in hepatoblasts in developing livers in a manner similar to our observations in adult mouse regenerating livers.

DISCUSSION

The findings from the present study demonstrate that DLK1 is selectively expressed in HSCs in the adult liver and up-regulated in HSC activation in culture, experimental liver fibrosis, and regeneration. *Dlk1* knockdown reverses activated HSCs to fat-storing quiescent cells via epigenetic derepression of *Pparγ* and restored expression of PPARγ in a manner dependent on suppression of canonical Wnts. From the established function of DLK1 as an antiadipogenic mediator (19, 21), this finding further enforces the concept that the loss of adipogenic regulation underlies a shift of HSC cell fate to myofibroblastic cells (3–9). A recent publication reports the causal role of DLK1 in HSC activation and the efficacy of *Dlk1* silencing for attenuating experimental fibrosis induced by CCl_4 (44). The findings presented here provide the epigenetic basis for the observed anti-fibrotic efficacy of *Dlk1* silencing involving HSC fate regulation. However, activation of HSCs has multidimensional functions in a wound-healing response of the liver including their contribution to liver regeneration. Indeed, the present study identifies DLK1 as a novel, early mediator of liver regeneration in the PH model. Thus, it may not be logically correct to blindly target DLK1 or HSC activation for a therapeutic purpose for liver disease as it may potentially impairs a regenerative response.

In liver regeneration after PH, HCs which normally do not express *Dlk1* up-regulate expression of this gene. This is consistent with DLK1 expression by embryonic hepatoblasts (27). Addition of anti-DLK antibody suppresses proliferation and *Dlk1* expression by PH HCs co-cultured with HSCs, suggesting a paracrine and/or autocrine mode of action. Because we also utilized the no-contact co-culture model, these results suggest that the cross-talk effects must be mediated via a cleaved soluble form as shown for regulation of adipocyte differentiation (29). Further, our results also demonstrate a self-inductive effect of DLK1 on *Dlk1* transcription (Fig. 3*E*), strengthening the possibility that HSC-derived DLK autoinduces its expression in HSCs while having the same inductive effect on HCs. It is also possible that DLK1 up-regulates other mediators which in turn renders proliferative signals in HCs. DLK1 positively cross-interacts with Wnts, necdin, and Shh (Fig. 3, *A–D*). After PH *in vivo*, induction of these morphogens lags behind the early *Dlk1* up-regulation in liver regeneration (Fig. 4*A*), suggesting that they may be downstream effectors of DLK1 in this model. The *in vivo* neutralization experiment shows significant inhibitory effects of HC DNA synthesis and liver growth during early liver regeneration. This inhibition is concomitant with diminished early regenerative signals such as decreased p-ERK1/2, p-AKT, and cyclins/CDKs. The HC mitogens *Wnt10b* and *Ptn* are down-regulated by anti-DLK1 antibody treatment *in vivo* (Fig. 5*A*) or *ex vivo* (Fig. 5*D*). Reduced levels of stabilized β-catenin by the antibody treatment are indicative of suppressed canonical Wnt signaling, which in turn may attenuate growth signaling such as p-ERK and p-AKT. Certainly, some of cell cycle genes such as *CyclinD1* are direct targets of canonical Wnts. Further, our results from the cross-culture experiment with Sham HCs and PH HSCs, strongly suggest that HSC-derived DLK1 induces the DLK1-Wnt10b pathway in HC as a mitogenic mechanism. However, other mediators may still be downstream of DLK1 in HCs and HSCs to participate in liver regeneration including *Ptn* and *p75Ntr*.

The anti-DLK1 antibody inhibitory effect on liver regeneration was transient and appeared to dissipate in the later time points. This may be due to a transient or incomplete neutralization of DLK1 by a single injection of the antibody at 6 h

FIGURE 6. *A*, chicken embryonic liver at E5 shows expression of desmin, αSMA, and DLK1 in HSCs surrounding islands or codes of hepatoblasts as detected by immunohistochemistry. Diffuse staining of DLK1 in a subpopulation of hepatoblasts is also evident. Magnification, ×200. *B*, immunohistochemistry of E9.5, E13.5, and E17.5 mouse embryos. In E9.5 embryos, DLK1 is expressed in both the foregut endoderm (*fg*) and $WT1^+$ septum transversum mesenchyme (*stm*). *h*, heart. In E13.5 embryos, DLK1 is expressed in $albumin^+$ hepatoblasts and $ALCAM^+$ mesothelial cells (*arrowhead*) and submesothelial cells (*arrows*) at the liver surface. Some $desmin^+$ HSCs and perivascular mesenchymal cells express DLK1 (*arrows*). In E17.5 embryos, expression of DLK1 becomes weak in hepatoblasts but persists in $ALCAM^+$ mesothelial cells (*arrowhead*) and submesothelial cells (*arrow*). Some $desmin^+$ HSCs and $p75Ntr^+$ Sma^+ perivascular mesenchymal cells (*arrows*) express DLK1. The nuclei were counterstained with DAPI. (Original blots that generated this figure are shown in suppl. Fig. S1.) *C*, FACS of GFP^+ cells from E13.5 embryonic or adult livers of the GFP-Coll mice. WT littermates were used as negative controls. GFP^+ populations were sorted for mRNA expression analysis. *D*, quantitative PCR of liver cells separated by FACS. The expression values were normalized against *Gapdh*. The GFP^+ populations from E13.5 or adult livers enrich expression of desmin and Col1a1. The E13.5 GFP^+ cells strongly express Dlk1, Lhx2, and Ptn compared with the adult GFP^+ cells. **, $p < 0.01$ compared with the E13.5 GFP^+ cells.

post-PH or a possible compensatory mechanism which has restored a normal regenerative activity. Nonetheless, our study is the first to identify the pivotal role of HSC-derived DLK1 in promoting HC proliferation and liver regeneration during the early phase following PH most likely via the DLK-Wnt10b pathway.

Our DLK1 expression analysis in embryonic livers also demonstrates the expression of this protein by HSCs in chicken embryos and by HSC precursors (mesothelial and submesothelial cells) and HSCs in mouse embryos along with the expression by hepatoblasts, establishing an observation parallel to what we have shown in adult liver regeneration. This raises an intriguing possibility that paracrine-autocrine loops of DLK1 may also participate in liver development. It is also possible that hepatocyte-derived DLK1 induces DLK1 expression by HSCs in liver regeneration. This paradigm has recently been proposed for CCl_4-induced liver fibrosis (44). In that study, no or minimal expression of *Dlk1* mRNA is detected in HSCs in sharp contrast to higher levels of expression in HSCs than hepatocytes isolated at day 1 after PH (Fig. 4*B*). HSCs isolated from CCl_4-induced and cholestatic liver fibrosis show induction of *Dlk1* mRNA (Fig. 1*C*). Our cross-culture experiment also demonstrates induction of *Dlk1* in hepatocytes from Sham-operated mice (which express no or minimal *Dlk1*) co-cultured with HSCs from PH mice expressing abundant *Dlk1* and abrogation of this effect with anti-DLK1 antibody (Fig. 5*D*). Thus, we present compelling evidence that HSCs up-regulates *Dlk1* in activation in culture as well as fibrosis and regeneration models. Reasons for this discrepancy are not known presently.

Global *Dlk1* knock-out mice may be considered for testing this morphogen in liver development and regeneration. *Dlk1* knock-out mice have pre- and postnatal growth retardation with skeletal malformation (45), but liver phenotype has not been examined. These mice also exhibit hyperlipidemia and increased adiposity (45). Because these metabolic complications may present confounding effects on assessment of liver regeneration, cell type-specific *Dlk1* ablation appears a most logical approach that would also provide more insights into HSC-hepatocyte cross-talk.

In conclusion, our study demonstrates for the first time that HSCs are the primary source of DLK1 in normal adult liver and *Dlk1* induction has a causal role in myofibroblastic trans-differentiation of HSCs via epigenetic repression of *Pparγ* involving canonical Wnt pathway. DLK1 induced in activated HSCs has a growth promoting effect on HC in liver regeneration via its paracrine and self-inductive interactions with the target cells. Detailed investigation of DLK1-mediated mesenchymal-epithelial interactions may disclose potential therapeutic targets to maximize beneficial effects on chronic liver disease.

REFERENCES

1. Friedman, S. L. (2008) Hepatic stellate cells: protean, multifunctional, and enigmatic cells of the liver. *Physiol. Rev.* **88,** 125–172
2. Brenner, D. A. (2009) Molecular pathogenesis of liver fibrosis. *Trans. Am. Clin. Climatol. Assoc.* **120,** 361–368
3. Hazra, S., Xiong, S., Wang, J., Rippe, R. A., Krishna, V., Chatterjee, K., and Tsukamoto, H. (2004) Peroxisome proliferator-activated receptor γ induces a phenotypic switch from activated to quiescent hepatic stellate cells. *J. Biol. Chem.* **279,** 11392–11401
4. She, H., Xiong, S., Hazra, S., and Tsukamoto, H. (2005) Adipogenic transcriptional regulation of hepatic stellate cells. *J. Biol. Chem.* **280,** 4959–4967
5. Miyahara, T., Schrum, L., Rippe, R., Xiong, S., Yee, H. F., Jr., Motomura, K., Anania, F. A., Willson, T. M., and Tsukamoto, H. (2000) Peroxisome proliferator-activated receptors and hepatic stellate cell activation. *J. Biol. Chem.* **275,** 35715–35722
6. Cheng, J. H., She, H., Han, Y. P., Wang, J., Xiong, S., Asahina, K., and Tsukamoto, H. (2008) Wnt antagonism inhibits hepatic stellate cell activation and liver fibrosis. *Am. J. Physiol. Gastrointest. Liver Physiol.* **294,** G39–49
7. Ross, S. E., Hemati, N., Longo, K. A., Bennett, C. N., Lucas, P. C., Erickson, R. L., and MacDougald, O. A. (2000) Inhibition of adipogenesis by Wnt signaling. *Science* **289,** 950–953
8. Zhu, N. L., Wang, J., and Tsukamoto, H. (2010) The necdin-Wnt pathway causes epigenetic peroxisome proliferator-activated receptor γ repression in hepatic stellate cells. *J. Biol. Chem.* **285,** 30463–30471
9. Mann, J., Chu, D. C., Maxwell, A., Oakley, F., Zhu, N. L., Tsukamoto, H., and Mann, D. A. (2010) MeCP2 controls an epigenetic pathway that promotes myofibroblast transdifferentiation and fibrosis. *Gastroenterology* **138,** 705–714
10. Passino, M. A., Adams, R. A., Sikorski, S. L., and Akassoglou, K. (2007) Regulation of hepatic stellate cell differentiation by the neurotrophin receptor p75NTR. *Science* **315,** 1853–1856
11. Asahina, K., Sato, H., Yamasaki, C., Kataoka, M., Shiokawa, M., Katayama, S., Tateno, C., and Yoshizato, K. (2002) Pleiotrophin/heparin-binding growth-associated molecule as a mitogen of rat hepatocytes and its role in regeneration and development of liver. *Am. J. Pathol.* **160,** 2191–2205
12. Watanabe, S., Hirose, M., Wang, X. E., Ikejima, K., Oide, H., Kitamura, T., Takei, Y., Miyazaki, A., and Sato, N. (1998) A novel hepatic stellate (Ito) cell-derived protein, epimorphin, plays a key role in the late stages of liver regeneration. *Biochem. Biophys. Res. Commun.* **250,** 486–490
13. Higashi, N., Sato, M., Kojima, N., Irie, T., Kawamura, K., Mabuchi, A., and Senoo, H. (2005) Vitamin A storage in hepatic stellate cells in the regenerating rat liver: with special reference to zonal heterogeneity. *Anat. Rec. A Discov. Mol. Cell Evol. Biol.* **286,** 899–907
14. Asai, K., Tamakawa, S., Yamamoto, M., Yoshie, M., Tokusashi, Y., Yaginuma, Y., Kasai, S., and Ogawa, K. (2006) Activated hepatic stellate cells overexpress p75NTR after partial hepatectomy and undergo apoptosis on nerve growth factor stimulation. *Liver Int.* **26,** 595–603
15. Enzan, H., Himeno, H., Iwamura, S., Onishi, S., Saibara, T., Yamamoto, Y., and Hara, H. (1994) α-Smooth muscle actin-positive perisinusoidal stromal cells in human hepatocellular carcinoma. *Hepatology* **19,** 895–903
16. Olaso, E., Salado, C., Egilegor, E., Gutierrez, V., Santisteban, A., Sancho-Bru, P., Friedman, S. L., and Vidal-Vanaclocha, F. (2003) Proangiogenic role of tumor-activated hepatic stellate cells in experimental melanoma metastasis. *Hepatology* **37,** 674–685
17. Olaso, E., Santisteban, A., Bidaurrazaga, J., Gressner, A. M., Rosenbaum, J., and Vidal-Vanaclocha, F. (1997) Tumor-dependent activation of rodent hepatic stellate cells during experimental melanoma metastasis. *Hepatology* **26,** 634–642
18. Bauer, S. R., Ruiz-Hidalgo, M. J., Rudikoff, E. K., Goldstein, J., and Laborda, J. (1998) Modulated expression of the epidermal growth factor-like homeotic protein dlk influences stromal-cell-pre-B-cell interactions, stromal cell adipogenesis, and pre-B-cell interleukin-7 requirements. *Mol. Cell. Biol.* **18,** 5247–5255
19. Smas, C. M., Kachinskas, D., Liu, C. M., Xie, X., Dircks, L. K., and Sul, H. S. (1998) Transcriptional control of the *pref-1* gene in 3T3-L1 adipocyte differentiation: sequence requirement for differentiation-dependent suppression. *J. Biol. Chem.* **273,** 31751–31758
20. Garcés, C., Ruiz-Hidalgo, M. J., Bonvini, E., Goldstein, J., and Laborda, J. (1999) Adipocyte differentiation is modulated by secreted delta-like (dlk) variants and requires the expression of membrane-associated dlk. *Differentiation* **64,** 103–114
21. Smas, C. M., and Sul, H. S. (1993) Pref-1, a protein containing EGF-like repeats, inhibits adipocyte differentiation. *Cell* **73,** 725–734
22. Abdallah, B. M., Jensen, C. H., Gutierrez, G., Leslie, R. G., Jensen, T. G., and Kassem, M. (2004) Regulation of human skeletal stem cells differentiation

by Dlk1/Pref-1. *J. Bone Miner. Res.* **19,** 841–852
23. Abdallah, B. M., Ditzel, N., Mahmood, A., Isa, A., Traustadottir, G. A., Schilling, A. F., Ruiz-Hidalgo, M. J., Laborda, J., Amling, M., and Kassem, M. (2011) DLK1 is a novel regulator of bone mass that mediates estrogen deficiency-induced bone loss in mice. *J. Bone Miner. Res.* **26,** 1457–1471
24. Kawaguchi, D., Yoshimatsu, T., Hozumi, K., and Gotoh, Y. (2008) Selection of differentiating cells by different levels of delta-like 1 among neural precursor cells in the developing mouse telencephalon. *Development* **135,** 3849–3858
25. Floridon, C., Jensen, C. H., Thorsen, P., Nielsen, O., Sunde, L., Westergaard, J. G., Thomsen, S. G., and Teisner, B. (2000) Does fetal antigen 1 (FA1) identify cells with regenerative, endocrine and neuroendocrine potentials? A study of FA1 in embryonic, fetal, and placental tissue and in maternal circulation. *Differentiation* **66,** 49–59
26. Yanai, H., Nakamura, K., Hijioka, S., Kamei, A., Ikari, T., Ishikawa, Y., Shinozaki, E., Mizunuma, N., Hatake, K., and Miyajima, A. (2010) Dlk-1, a cell surface antigen on foetal hepatic stem/progenitor cells, is expressed in hepatocellular, colon, pancreas, and breast carcinomas at a high frequency. *J. Biochem.* **148,** 85–92
27. Tanimizu, N., Nishikawa, M., Saito, H., Tsujimura, T., and Miyajima, A. (2003) Isolation of hepatoblasts based on the expression of Dlk/Pref-1. *J. Cell Sci.* **116,** 1775–1786
28. Kim, Y., Lin, Q., Zelterman, D., and Yun, Z. (2009) Hypoxia-regulated delta-like 1 homologue enhances cancer cell stemness and tumorigenicity. *Cancer Res.* **69,** 9271–9280
29. Wang, Y., and Sul, H. S. (2006) Ectodomain shedding of preadipocyte factor 1 (Pref-1) by tumor necrosis factor α-converting enzyme (TACE) and inhibition of adipocyte differentiation. *Mol. Cell. Biol.* **26,** 5421–5435
30. Sánchez-Solana, B., Nueda, M. L., Ruvira, M. D., Ruiz-Hidalgo, M. J., Monsalve, E. M., Rivero, S., García-Ramírez, J. J., Díaz-Guerra, M. J., Baladrón, V., and Laborda, J. (2011) The EGF-like proteins DLK1 and DLK2 function as inhibitory non-canonical ligands of NOTCH1 receptor that modulate each other's activities. *Biochim. Biophys. Acta* **1813,** 1153–1164
31. Nueda, M. L., García-Ramírez, J. J., Laborda, J., and Baladrón, V. (2008) dlk1 specifically interacts with insulin-like growth factor binding protein 1 to modulate adipogenesis of 3T3-L1 cells. *J. Mol. Biol.* **379,** 428–442
32. Wang, Y., Zhao, L., Smas, C., and Sul, H. S. (2010) Pref-1 interacts with fibronectin to inhibit adipocyte differentiation. *Mol. Cell. Biol.* **30,** 3480–3492
33. Machida, K., Tsukamoto, H., Mkrtchyan, H., Duan, L., Dynnyk, A., Liu, H. M., Asahina, K., Govindarajan, S., Ray, R., Ou, J. H., Seki, E., Deshaies, R., Miyake, K., and Lai, M. M. (2009) Toll-like receptor 4 mediates synergism between alcohol and HCV in hepatic oncogenesis involving stem cell marker Nanog. *Proc. Natl. Acad. Sci. U.S.A.* **106,** 1548–1553
34. Magness, S. T., Bataller, R., Yang, L., and Brenner, D. A. (2004) A dual reporter gene transgenic mouse demonstrates heterogeneity in hepatic fibrogenic cell populations. *Hepatology* **40,** 1151–1159
35. Sung, C. K., She, H., Xiong, S., and Tsukamoto, H. (2004) Tumor necrosis factor-α inhibits peroxisome proliferator-activated receptor-γ activity at a posttranslational level in hepatic stellate cells. *Am. J. Physiol. Gastrointest. Liver Physiol.* **286,** G722–729
36. Xiong, S., She, H., Takeuchi, H., Han, B., Engelhardt, J. F., Barton, C. H., Zandi, E., Giulivi, C., and Tsukamoto, H. (2003) Signaling role of intracellular iron in NF-κB activation. *J. Biol. Chem.* **278,** 17646–17654
37. Tokairin, T., Nishikawa, Y., Doi, Y., Watanabe, H., Yoshioka, T., Su, M., Omori, Y., and Enomoto, K. (2002) A highly specific isolation of rat sinusoidal endothelial cells by the immunomagnetic bead method using SE-1 monoclonal antibody. *J. Hepatol.* **36,** 725–733
38. Asahina, K., Tsai, S. Y., Li, P., Ishii, M., Maxson, R. E., Jr., Sucov, H. M., and Tsukamoto, H. (2009) Mesenchymal origin of hepatic stellate cells, submesothelial cells, and perivascular mesenchymal cells during mouse liver development. *Hepatology* **49,** 998–1011
39. Maher, J. J., Bissell, D. M., Friedman, S. L., and Roll, F. J. (1988) Collagen measured in primary cultures of normal rat hepatocytes derives from lipocytes within the monolayer. *J. Clin. Invest.* **82,** 450–459
40. Smas, C. M., Green, D., and Sul, H. S. (1994) Structural characterization and alternate splicing of the gene encoding the preadipocyte EGF-like protein pref-1. *Biochemistry* **33,** 9257–9265
41. Smas, C. M., Chen, L., and Sul, H. S. (1997) Cleavage of membrane-associated pref-1 generates a soluble inhibitor of adipocyte differentiation. *Mol. Cell. Biol.* **17,** 977–988
42. Yang, L., Wang, Y., Mao, H., Fleig, S., Omenetti, A., Brown, K. D., Sicklick, J. K., Li, Y. X., and Diehl, A. M. (2008) Sonic hedgehog is an autocrine viability factor for myofibroblastic hepatic stellate cells. *J. Hepatol.* **48,** 98–106
43. Asahina, K., Zhou, B., Pu, W. T., and Tsukamoto, H. (2011) Septum transversum-derived mesothelium gives rise to hepatic stellate cells and perivascular mesenchymal cells in developing mouse liver. *Hepatology* **53,** 983–995
44. Pan, R. L., Wang, P., Xiang, L. X., and Shao, J. Z. (2011) Delta-like 1 serves as a new target and contributor to liver fibrosis down-regulated by mesenchymal stem cell transplantation. *J. Biol. Chem.* **286,** 12340–12348
45. Moon, Y. S., Smas, C. M., Lee, K., Villena, J. A., Kim, K. H., Yun, E. J., and Sul, H. S. (2002) Mice lacking paternally expressed Pref-1/Dlk1 display growth retardation and accelerated adiposity. *Mol. Cell. Biol.* **22,** 5585–5592